Original Article

Journal of Intelligent Material Systems and Structures

Journal of Intelligent Material Systems and Structures
1–10

DOI: 10.1177/1045389X15571380
jim.sagepub.com
SAGE

Constitutive model for shape memory polymer based on the viscoelasticity and phase transition theories

Xiaogang Guo[1], Liwu Liu[2], Bo Zhou[3], Yanju Liu[2] and Jinsong Leng[4]

Abstract

As a kind of smart materials, shape memory polymer has covered broad applications for its shape memory effect. Precise description of the mechanical behaviors of shape memory polymer has been an urgent problem. Since the phase transition was a continuous time-dependent process, shape memory polymer was composed of several individual transition phases. Owing to the forming and dissolving of individual phases with the change in temperature, shape memory effect emerged. In this research, shape memory polymer was divided into different kinds of phases including frozen and active phases for its thermodynamics properties. Based on the viscoelasticity theory and phase transition theories, a new constitutive model for shape memory polymer which can explain the above assumptions was studied. In addition, a normal distribution model, which possesses less but physical meaning parameters, was proposed to describe the variation in the volume fraction in shape memory polymer during heating or cooling process.

Keywords

shape memory polymer, constitutive model, phase transition, viscoelasticity and phase transition theories

Introduction

Since the shape memory polymer (SMP) was discovered in 1980s, it has drawn much attention and has been vastly developed during the past decades (Ratna and Karger-Kocsis, 2007; Wei et al., 1998). SMP possesses the ability of returning from deformed shape to original shape under a reasonable stimulus such as temperature, light, electric field, magnetic field, pH, specific ions, or enzyme (Behl and Lendlein, 2007; Fei et al., 2012; Hu et al., 2012; Leng et al., 2011; Meng and Li, 2013; Xu et al., 2010). And the thermal-actuated SMP has been widely studied as a typical one. With the variation in temperature, the thermal–mechanical cycle of shape memory effect (SME) is as shown in Figure 1. Depending on the phase transition temperature T_g, the process can be classified into the following steps: (1) heat and deform SMP at a high temperature above T_g; (2) cool and remove the external force at a lower temperature; and (3) heat the pre-deformed SMP above T_g and then the polymer will recover to its original shape.

Compared with other smart materials such as shape memory alloy, SMP possesses the advantages of large deformation capacity, low density, and cost. However, the main drawbacks of SMP are their low actuation forces and long recovery time. For the sake of their low stiffness and strength, SMP composites, which were filled with particles, carbon nanotubes, and short fibers (Basit et al., 2012; Tan et al., 2014; Yu et al., 2013, 2014; Zhang and Li, 2013), were investigated. Now, SMP composites and their products such as deployable and morphing structures have been researched and developed (Leng et al., 2011; Liu et al., 2014; Meng and Hu, 2009).

In order to investigate the mechanical behaviors of SMP, various constitutive models and a large tensile, compression, torsion, and flexure experiments (Chen et al., 2014; Diani et al., 2012; Guo et al., 2014; Liu

[1]College of Aerospace and Civil Engineering, Harbin Engineering University, Harbin, China
[2]Department of Astronautical Science and Mechanics, Harbin Institute of Technology, Harbin, China
[3]College of Pipeline and Civil Engineering, China University of Petroleum, Qingdao, China
[4]Center for Composite Materials and Structures, Harbin Institute of Technology, Harbin, China

Corresponding authors:
Yanju Liu, Department of Astronautical Science and Mechanics, Harbin Institute of Technology, Harbin 150001, China.
Email: yj_liu@hit.edu.cn

Jinsong Leng, Center for Composite Materials and Structures, Harbin Institute of Technology, Harbin 150080, China.
Email: lengjs@hit.edu.cn

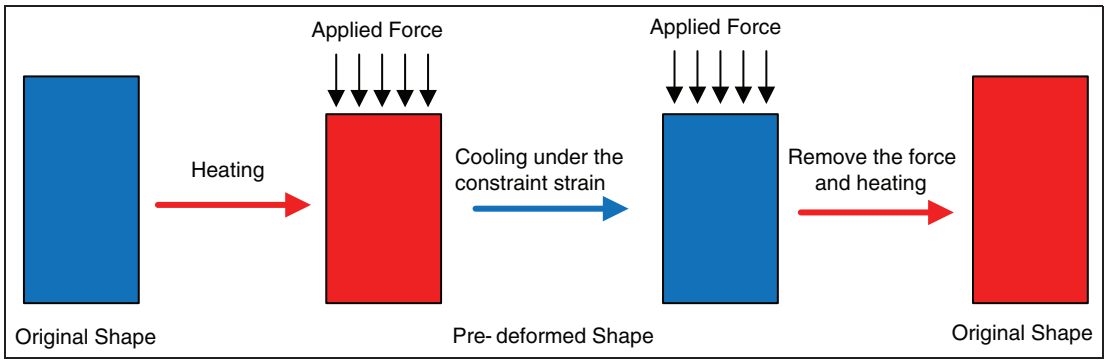

Figure 1. Schematic of phase transition in shape memory effect during typical thermal–mechanical cycle.

et al., 2006; Srivastava et al., 2010) were carried out. Tobushi et al. (1997) established a simple thermal–mechanical model describing the mechanical behaviors of the thermal-actuated polymer using a rheological model based on the viscoelasticity theory. Through taking nonlinear mechanical behaviors into account, a nonlinear one-dimensional (1D) constitutive model for SMP was proposed in 2001 (Tobushi et al., 2001). Considering the strain rate during the loading and unloading processes, Shim and Mohr (2011) built a new constitutive model which was composed of two Maxwell elements. Most of these modeling efforts have adopted rheological models consisting of spring, dashpot, and frictional elements in 1D constitutive models. Though these models are simple, they only agree qualitatively with the experimental results. In the constitutive model of SMP, the concept of phase transition was also used. Although there is a slight difference between physical nature of melting and glass transition, they both can explain SME for certain macroscopic characteristics. And the concept of phase transition is convenient for analyzing the mechanical behaviors of SMP (Long et al., 2010). Based on modeling the crystallization and taking the phase transition into account, several constitutive models for SMP were also developed. In 2006, a new thermal–mechanical model that divided the polymer into frozen and active phases was investigated, and a three-dimensional (3D) micromechanical constitutive model was built by Liu et al. (2006). In Liu et al.'s (2006) article, the strain of the materials was decomposed into mechanical strain, thermal strain, and storage strain which was the critical factor for the SME. And the active and frozen phases were all treated as elastic materials and could not describe the viscoelasticity of SMP at a constant loading condition and temperature. However, the SMP in this article was treated as the elastic materials, not time dependency materials (Baghani et al., 2012). Based on Liu et al.'s (2006) work and the experience of investigating the phase transition of shape memory alloys, Chen and Lagoudas (2008a, 2008b) studied the micromechanism of SME and created a 3D constitutive model for SMP under large deformation. Meanwhile, a constitutive model for crystallization of SMP was proposed and the interaction between original amorphous and semi-crystalline phase was also investigated (Barot et al., 2008). In order to explain the molecular mechanisms of the SME in amorphous SMPs, Nguyen et al. (2008) established a thermal-viscoelastic constitutive model and assumed that structural relaxation and stress relaxation were the key factors for SME. Taking the non-equilibrium relaxation processes into account, Westbrook et al. (2011) established a 3D finite deformation constitutive model for amorphous SMP. Based on micromechanics framework, Shojaei and Li (2013) developed a multi-scale theory, which links micro-scale and macro-scale constitutive behaviors of the polymers. For the sake of the influence of material parameters on the response characteristics of the constitutive model, Ghosh and Srinivasa (2013) proposed a 3D continuum two-network for a thermal–elastic response model of SMP. And during the last few years, a new phenomenon for SMP—multi-SMEs—was discovered by which SMP can memorize more than one temporary shape (Xie, 2010). And the research on the mechanisms of multi-SMEs was investigated (Yu et al., 2012).

The purpose of this article is to establish a constitutive model that can unify the linear elasticity and viscoelasticity into one equation. The concepts of phase transition and the theory of multi-SMEs were also considered and described. Using the four-element model, the mechanical behaviors of the individual transition phases were analyzed. The volume fractions of transition phases which can join them together were discussed, and a normal distributed equation that can simulate the change in these fractions in SMP during heating or cooling process was built. Finally, in order to confirm the parameters in this new constitutive model, the dynamic mechanical analysis (DMA) tests and creep experiments were also accomplished.

The phase transition in SMP

The phase transition process in SMP during heating or cooling is complex. Obviously, SMP consists of a lot of molecule chains with different lengths and angles.

Taking the pre-stress and storage energy into account, the entropy of each chain also differs from the others, as well as their phase transition temperatures. During cooling process from a high temperature, the phase transition will come out first in the molecule chain with higher entropy. That is, when cooled to a specific temperature, phase transition in the molecule chain will happen and the relevant parts will change from "active phase" to "frozen phase." Thus, the specific temperature is the phase transition temperature of those molecule chains. With the decrease in temperature, the molecule chain will shrink while the stiffness of SMP will increase. The shrinkage of the chain was due to the removal of residual stress formed in the polymer process step (shown in Figure 1). Based on the statistics, the molecule chains in SMP can be divided into several classes by their phase transition temperatures. The volume fraction of each active class can be expressed by ϕ_i while the one of frozen phase is ϕ_f. In this model, the variation in volume fraction controls the strain release and storage in thermomechanical cycle. And they can be defined as

$$\phi_f = \frac{V_f}{V} \quad \phi_i = \frac{V_i}{V} \quad \phi_f + \sum \phi_i = 1 \tag{1}$$

in which ϕ_f and ϕ_i are the volume fraction of frozen phase and ith relevant active phase, respectively. V is the total volume of the SMP. When the SMP is loaded during heating or cooling process, the strain energy will almost be absorbed by active phase for conformation rotation of the polymer. When cooled down to phase transition temperature, the phase transition will happen and the strain in ith active phase will also be stored as storage strain. Finally, the strain energy and deformation are almost stored in SMP even after unloading at a low temperature. During the recovery process, the strain energy and deformation stored in the ith active phase during loading and cooling process will release at its phase transformation temperature. Then, the deformed SMP will recover to its original shape. And the SME will emerge.

In addition, when a multi-load is applied on SMP at different temperatures, the mechanical strain caused by multi-stress will be stored in different active phases such as ith, jth, or kth. Thus, during the heating or recovery process, the storage strain in certain active phase will be released when these phases experience the relevant temperature again, which is the reason for multi-SMEs.

In addition, not only the storage strain but also the viscoelasticity behaviors of SMP such as stress relaxation play an important role on SME.

Based on the above discussions, the volume fraction of frozen phase and active phase is a very important parameter for SMP during phase transition process. The researches about this issue have been carried out, and kinds of models such as trigonometric function model and quadratic polynomial model have been built in order to indicate the relationship between the fraction and the temperature. But the cosine model consisted of two equations, so the slope of two equations at demarcation point T_g was not equal. The quadratic polynomial model built in 2006 was an empirical equation, whose two parameters were confirmed by fitting the experiment results.

In this article, a new volume fraction model that can indicate the phase transition accurately in a simple formation was brought up and the volume fraction of the SMP during phase transition can be given by

$$\phi_f = \int_{Ts}^{T} \frac{1}{S\sqrt{2\pi}} e^{-\frac{(T-T_g)^2}{2S^2}} dT \tag{2}$$

in which S is the variance of the normal distribution function and can be expressed as

$$S = \frac{T_f - T_g}{n} \tag{3}$$

where n is a constant. T_g is the average value of the normal distribution and it is also the temperature at which the volume fraction is 0.5.

As indicated in Figure 2, with the increase in temperature, the volume fraction of frozen phase decreases nonlinearly, the rate of which grows rapidly until to the phase transition temperature T_g. The phase transition temperature is about 320 K, while the starting temperature is 273 K. When T/T_g reaches 1.04, at which the environment temperature is 358 K, the phase transition ends and the volume fraction of frozen phase will decrease to 0. Based on the comparison results, the normal distribution function can describe the variation in the volume fraction accurately.

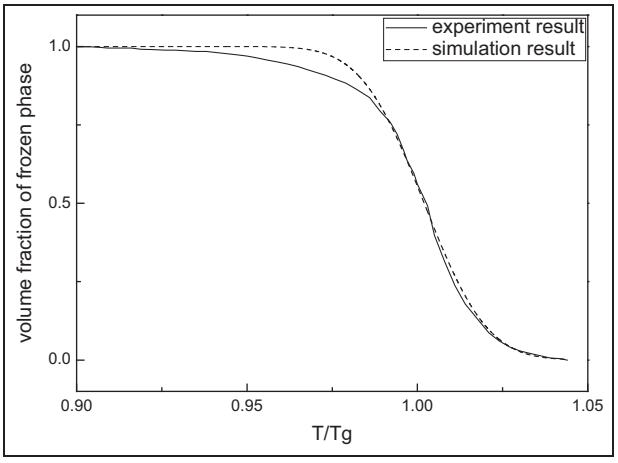

Figure 2. Comparisons with simulation results using experiment results (Liu et al., 2006) of volume fraction.

A new constitutive model for SME

In the ith active phase, the strain is decomposed into two parts: thermal expansion strain ε_i^T and mechanical strain ε_i^m. Thus, the total strain of active phase can be expressed as

$$\varepsilon_i = \varepsilon_i^m + \varepsilon_i^T \tag{4}$$

While the strain in frozen phase is constituted by storage strain ε^S, mechanical strain ε_f^m and thermal expansion strain ε_f^T

$$\varepsilon_f = \varepsilon^S + \varepsilon_f^m + \varepsilon_f^T \tag{5}$$

So, the strain of SMP during heating or cooling process can be finally shown as

$$\varepsilon = \phi_f \varepsilon_f + \Sigma \phi_i \varepsilon_i \tag{6}$$

And the total thermal expansion strain ε^T, which is divided into several parts, is given as

$$\varepsilon^T = \phi_f \varepsilon_f^T + \phi_i \varepsilon_i^T = (\phi_f \alpha_f + \phi_i \alpha_i)\Delta T \tag{7}$$

where ΔT is the change in temperature and α_i and α_f are the thermal expansion coefficients of ith active and frozen phases, respectively.

In order to describe the mechanical behavior of SMP, the 1D rheological model for the new constitutive model is shown in Figure 3. G_f and G_f' represent the elastic modulus of frozen phase model and G_i and G_i' are of the ith phase model. η_f and η_f' are the viscosity coefficients of frozen phase model, while the coefficient of ith phase model can be expressed by η_i and η_i'.

Due to the viscoelasticity behaviors of active and frozen phases, the mechanical strains ε_i^m and ε_f^m are indicated as

$$\varepsilon_i^m = \sigma J_i(T,t) = \sigma\left(\frac{1}{G_i} + \frac{1}{G_i'}(1 - e^{-t/\tau_i'}) + \frac{t}{\eta_i}\right)$$
$$\varepsilon_f^m = \sigma J_f(T,t) = \sigma\left(\frac{1}{G_f} + \frac{1}{G_f'}(1 - e^{-t/\tau_f'}) + \frac{t}{\eta f}\right)$$

In equation (8), the parameter τ' is the retardation time and can be expressed by G' and η'. That is

$$\tau' = \frac{\eta'}{G'} \tag{9}$$

So, the strain in SMP which is the function of time and temperature can be defined as

$$\varepsilon = \phi_f(\varepsilon^S + \varepsilon_f^m) + \sum_1^n \phi_i \varepsilon_i^m + \varepsilon^T = \sigma(\phi_f(T)J_f(T,t) + \sum_1^n \phi_i(T)J_i(T,t) + \phi_f \varepsilon^S + \varepsilon^T \tag{10}$$

For multi-load conditions, the strain in the SMP can be given as

$$\varepsilon = \sum_1^m \phi_f(T)J_f(T, t - t_j)\sigma_j + \sum_1^m \sum_1^n \phi_i(T)J_i\big(T, t - t_j\big)\big) + \phi_f \varepsilon^S + \varepsilon^T \tag{11}$$

Here, t_j is the time when σ_j applied during the loading or recovery process.

The phase transition process in SMP is continuous definitely during cooling or heating process. In order to simplify calculations, we assume that

$$J_i(T,t) = J_a(T,t), \quad \alpha_i = \alpha_a \tag{12}$$

The thermal expansion strain ε^T can be finally expressed as

$$\varepsilon^T = \phi_f \varepsilon_f^T + \Sigma \phi_i \varepsilon_i^T = \int_{T_0}^{T} (\phi_f \alpha_f + \phi_a \alpha_a) dT \tag{13}$$

And the mechanical strain in active phase ε_a^m can be simply expressed as

$$\varepsilon_a^m = \varepsilon_i^m = \sigma J_a(T,t) \tag{14}$$

in which $J_a(T,t)$ is the creep compliance of active phase

$$J_a(T,t) = \frac{1}{G_a} + \frac{1}{G_a'}(1 - e^{-t/\tau_a'}) + \frac{t}{\eta_a} \tag{15}$$

Incorporating equations (1) and (14) into equation (10), we have

$$\varepsilon = \phi_f(\varepsilon^S + \varepsilon_f^m) + \sum_1^n \phi_i \varepsilon_a^m + \varepsilon^T = \sigma\big(\phi_f(T)J_f(T,t) + \phi_a(T)J_a(T,t)\big) + \phi_f \varepsilon^S + \varepsilon^T \tag{16}$$

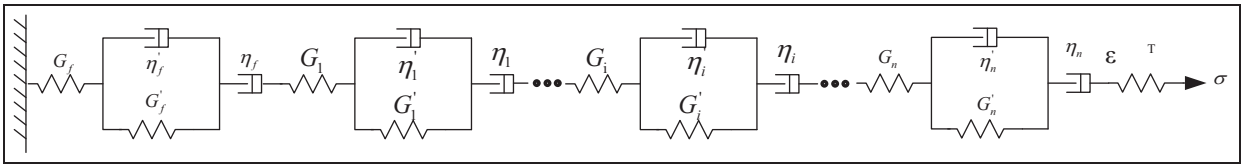

Figure 3. 1D rheological representations for the developed model.

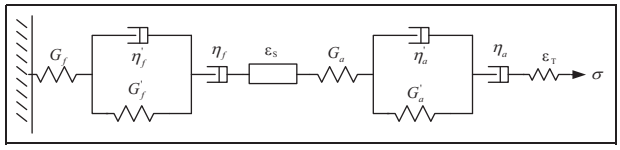

Figure 4. A simplified 1D rheological representation for the developed model.

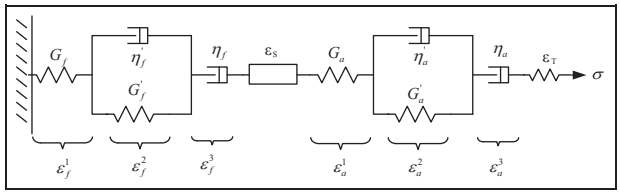

Figure 5. A simplified 1D rheological representation for the developed model with several decomposed strains.

Here, ϕ_a, G_a, τ_a', and η_a are the volume fraction, elastic modulus, retardation time, and viscosity coefficient of active phase, while ϕ_f, G_f, τ_f', and η_f are the correspondent parameters of frozen phase, respectively.

During cooling process with a constant stress or strain, the phase transition comes out and the mechanical strain in ith active phase will be stored in frozen phase. So, the storage strain ε^S is given as

$$\varepsilon^S = \frac{1}{V_f}\int_0^{V_f} \varepsilon_a^m dv = \frac{V}{V_f}\int_0^{V_f} \varepsilon_a^m d\frac{v}{V} = \frac{1}{\phi_f}\int_0^{\phi_f} \varepsilon_a^m d\phi \tag{17}$$

Equation (16), which combines viscoelasticity theory and phase transition model, is the constitutive model for SMP during cooling or heating. In this theory, the above viscoelasticity model shown in Figure 3 was replaced by a simplified developed model which consisted of only two phases—frozen phase and active phase (Figure 4). Moreover, the two distinct phases possess the equal stress but different strains.

Generally, stress relaxation will happen during cooling process at a constant strain ε_0. And with the decrease in temperature, the increase in elastic modulus will play an important role compared with stress relaxation. Meanwhile, the active and frozen phases during cooling process were also treated as elastomeric. And during cooling process, the mechanical strain will be stored due to phase transition and becomes an irrecoverable deformation which cannot undertake stress. Thus, the stress σ_m used for maintaining the deformation which is the function of temperature can be finally expressed as

$$\sigma_m = G(T)(\varepsilon^0 - \varepsilon^S - \varepsilon^T) \tag{18}$$

where $G(T)$ is the elastic modulus of SMP during cooling process. In this model, the elastic modulus of SMP $G(T)$ can be represented by the elastic modulus of frozen phase G_f and active phase G_a

$$\frac{1}{G(T)} = \frac{\phi_a}{G_a} + \frac{\phi_f}{G_f} \tag{19}$$

As Liu indicated, G_f is a constant and G_a possesses a linear relationship with temperature

$$G_f = \text{Constant},\ G_a = 3\,NKT \tag{20}$$

In order to explore the mechanical behaviors during recovery process, the total strain of SMP was decomposed into several parts (as shown in Figure 5)

$$\begin{aligned}\varepsilon &= \varepsilon_f + \varepsilon_a + \varepsilon^S + \varepsilon^T \\ &= \varepsilon_f^1 + \varepsilon_f^2 + \varepsilon_f^3 + \varepsilon_a^1 + \varepsilon_a^2 + \varepsilon_a^3 + \varepsilon^S + \varepsilon^T\end{aligned} \tag{21}$$

Thus, the storage strain ε^S will not undertake the load so is the thermal expansion strain ε^T. Therefore, when the load is constant, these strains can be expressed as follows

$$\begin{cases}\sigma = G_f\varepsilon_f^1 \\ \sigma = G_f'\varepsilon_f^2 + \eta_f'\frac{d\varepsilon_f^2}{dt} \\ \sigma = \eta_f\frac{d\varepsilon_f^3}{dt}\end{cases}\quad\begin{cases}\sigma = G_a\varepsilon_a^1 \\ \sigma = G_a'\varepsilon_a^2 + \eta_a'\frac{d\varepsilon_a^2}{dt} \\ \sigma = \eta_a\frac{d\varepsilon_a^3}{dt}\end{cases} \tag{22}$$

During the recovery process, the stress in the SMP is 0 obviously and the boundary conditions would be predicted that $d\sigma/dt = 0$ and $\sigma = 0$. So, the strain in SMP can be rewritten as

$$\begin{cases}0 = G_f\varepsilon_f^1 \\ 0 = G_f'\varepsilon_f^2 + \eta_f'\frac{d\varepsilon_f^2}{dt} \\ 0 = \eta_f\frac{d\varepsilon_f^3}{dt}\end{cases}\quad\begin{cases}0 = G_a\varepsilon_a^1 \\ 0 = G_a'\varepsilon_a^2 + \eta_a'\frac{d\varepsilon_a^2}{dt} \\ 0 = \eta_a\frac{d\varepsilon_a^3}{dt}\end{cases} \tag{23}$$

And the total strain during recover process can be finally indicated as

$$\begin{aligned}\varepsilon_{rec} &= \varepsilon_f^2 + \varepsilon_a^2 + \phi_a(T)\varepsilon_0^S + \varepsilon^T \\ &= \varepsilon_0(\phi_f e^{-t/\tau_f} + \phi_a e^{-t/\tau_a}) + \phi_a(T)\varepsilon_0^S + \varepsilon^T\end{aligned} \tag{24}$$

Here, ε_0 is the strain that formed during cooling process due to the molecule relaxation. σ_0 and G are the original applied stress and elastic modulus, respectively. The parameter $\phi_a(T)\varepsilon_0^S$ represents the released storage strain at temperature T, while ε_0^S is the original storage strain before recovery process. When the deformed specimen was heated at a low temperature, the stored strain was only released partly and the specimen could not recover to its original shape completely. And the residual strain will depend on the value of active and frozen phases at that temperature.

In the creep experiments at a constant temperature, the viscous flow rarely happens and the storage strain is also 0. So, the strain in frozen phase ε_f^c and active phase ε_a^c can be, respectively, expressed as

$$\varepsilon_f^c = \frac{\sigma}{G_f} + \frac{\sigma}{G_f'}(1 - e^{-(t/\tau_f)})$$
$$\varepsilon_a^c = \frac{\sigma}{G_a} + \frac{\sigma}{G_a'}(1 - e^{-(t/\tau_a)})$$

At the beginning of the creep, the power exponent on the right side of equation (25) is nearly 1. So, the strains in frozen phase ε_f^c and active phase ε_a^c are all linear as time goes on

$$\varepsilon_c = \phi_f \varepsilon_f^c + \phi_a \varepsilon_a^c = \phi_f \frac{\sigma}{G_f} + \phi_a \frac{\sigma}{G_a} \tag{26}$$

When the time t is infinitely great, the power exponent is approximately 0 for the measurements of the parameters τ_f and τ_a

$$\varepsilon_c = \phi_f \varepsilon_f^c + \phi_a \varepsilon_a^c = \phi_f \left(\frac{\sigma}{G_f} + \frac{\sigma}{G_f'}\right) + \phi_a \left(\frac{\sigma}{G_a} + \frac{\sigma}{G_a'}\right) \tag{27}$$

Experimental and simulated results

In order to investigate the mechanical behaviors of SMP and the correctness of the new constitutive model built in this article, several experiments such as the creep experiments and DMA test were completed. In the section of DMA tests, the phase transition temperature of SMP was obtained. And the experimental results are also shown in Figure 6. And the accuracy of the phase transition model (equation (2)) was verified in the section of comparison between the simulated and experimental results from Liu et al.'s (2006) research work. Finally, the creep experiments under a constant stress and temperature (348 and 360 K) were conducted to verify the precision of constitutive model built in this article. In this article, all the specimens used for mechanical experiments were made of styrene, one typical kind of SMP.

DMA test

Figure 6 is the DMA test results of SMP. The experiment sample was cut into pieces of 19 mm × 3 mm × 2 mm using laser cutting machine at the environment temperature of 300 K. The experimental frequency and temperature range were 1 Hz and from 293 to 460 K, respectively. As indicated in Figure 6, the relationship between temperature and elastic modulus was obtained. The glass transition temperature T_g is about 340 K.

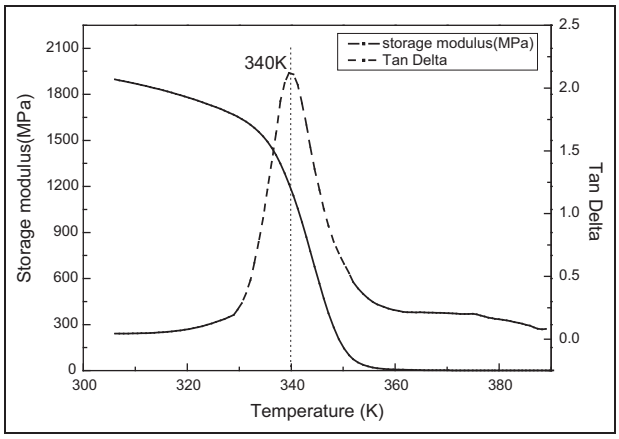

Figure 6. Dynamic mechanical analysis test results of shape memory polymer.

Table 1. Parameters of styrene obtained through creep experiments at different temperatures.

T (K)	E (MPa)	J (MPa^{-1})	τ (s)
348	420	1.67	180
360	10	1.75	73
368	1	3.9	65

Creep experiment at a constant temperature

For the sake of determining the parameters in equations (8) and (15), the creep experiments at several high temperatures T_g were finished.

The creep experiments were conducted using ZWICK/Z010 at several constant temperatures. The SMP was first preheated for about 30 min at the target temperature before loading. The stress at 348 and 360 K was 0.05 MPa, while the stress at 368 K was 0.01 MPa. The experiment results are shown in Figures 7 to 9. According to the DMA test and creep experiments, several parameters of SMP at different temperatures can be obtained and are listed in Table 1.

Though it is difficult to measure the retardation and relaxation time at a low temperature, these two parameters can be indirectly achieved following the Arrhenius-type behavior (O'Connell and McKenna, 1999)

$$\ln \alpha_T(T) = -\frac{AF_c}{k_B}\left(\frac{1}{T} - \frac{1}{T_g}\right) \tag{28}$$

in which k_B is the Boltzmann constant, A is a constant, and F_c is the configurationally free energy which is the reciprocal of the configurationally entropy S_c. Significantly, F_c is a constant below the glass transition temperature. α_T is the time–temperature superposition shift factor

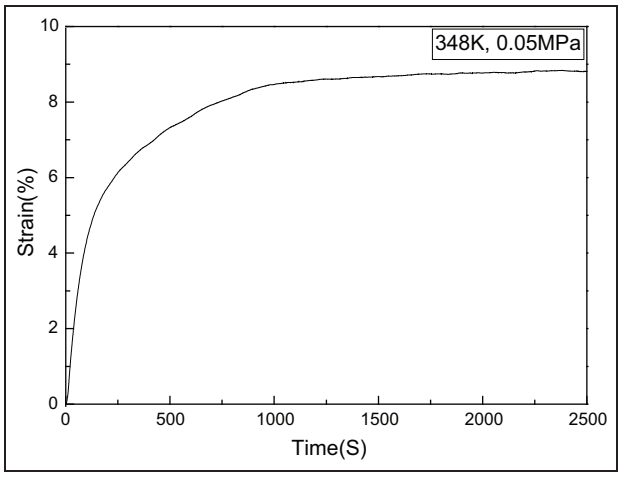

Figure 7. Creep behavior of shape memory polymer at 348 K and 0.05 MPa.

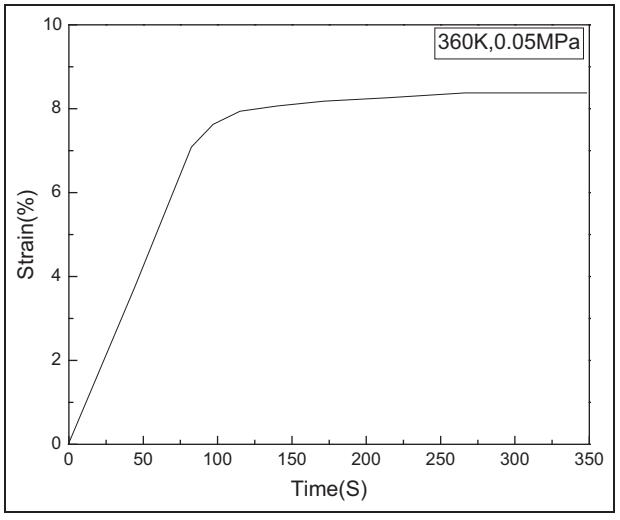

Figure 8. Creep behavior of shape memory polymer at 360 K and 0.05 MPa.

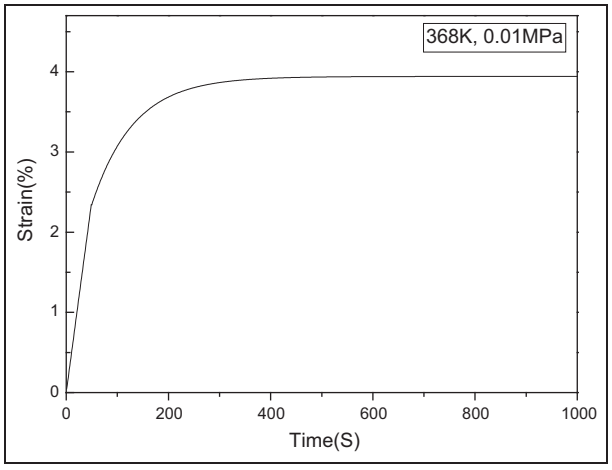

Figure 9. Creep behavior of shape memory polymer at 368 K and 0.01 MPa.

$$\alpha_T = \frac{\tau}{\tau_0} \tag{29}$$

So, the retardation time in active phase at a room temperature can be indirectly obtained.

In this model, there were several parameters to be determined through the experiments at high or low temperature to describe the mechanical behaviors of SMP. G_a and G_f are the elastic moduli of active and frozen phases, which can be obtained from the tensile experiments at high and low temperatures with a constant strain rate. τ_a' and η_a are the retardation time and viscosity coefficient of active phase, while τ_f' and η_f are the correspondent parameters of frozen phase, respectively. G_a', τ_a', and η_a can be measured through the creep experiments at a high temperature, while τ_f' and η_f were measured at a low temperature which will cost a lot of time. So, in this model, the Arrhenius-type equation was proposed to estimate the values of τ_f' and η_f. Besides, the phase transition temperature T_g would be obtained by DMA tests. And these parameters of SMP used in this constitutive model are listed in Table 2.

As shown in Table 2, the retardation time and viscosity coefficient of frozen phase are nearly 10^7–10^8 times than those of active phase. And the elasticity characters play a more important role than viscoelasticity characters in frozen phase. For simplification, frozen phase is analyzed as elastomeric materials with an elastic modulus G_f (as shown in Figure 10). So frozen phase also can be interpreted as the phase used to fix geometry of the materials.

Based on the theories established in this article, the simulated results of creep and recovery processes were obtained. In addition, the comparison results between simulation and experiments at different temperatures (348, 360, and 368 K) are indicated in Figures 11 to 13. As the creep results show, the mechanical property of SMP was elastic at the beginning of loading process. As time goes on, the viscoelasticity of SMP gradually emerges and the relationship between strain and time is nonlinear. The creep compliance can be obtained if plenty of time condition is allowed. As the comparison results show, the constitutive model built in this article can describe the creep behaviors of styrene precisely, especially at 348 and 368 K.

Cooling experiment under a constant strain

In order to investigate the mechanical behavior of SMP during cooling process, the cooling experiments at a constant strain were carried out. The samples were first stretched to an elongation of 30% using a 50%/s strain rate at the temperature of 381 K ($T_g + 20$ K). The respective temperature was kept constant for about 60 s before cooling down to the room temperature (with a cooling rate of 0.8 K/min).

Table 2. Summary of shape memory polymer and simulation parameters.

G_a (MPa)	G_a' (MPa)	G_f (MPa)	η_a (MPa s)	η_f (MPa s)	τ_a' (s)
0.85	0.26	1825	1.68×10^6	6.1×10^9	71
τ_f' (s)	T_g (K)	$-AF_ck_B^{-1}$	α_f (10^{-4}/K)	α_a (10^{-4}/K)	
4.75×10^6	340	18,000	0.7	1.4	

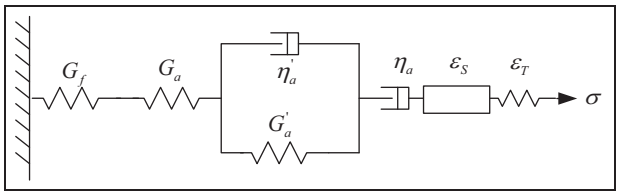

Figure 10. A simplified 1D rheological representation considering frozen phase as elastomer.

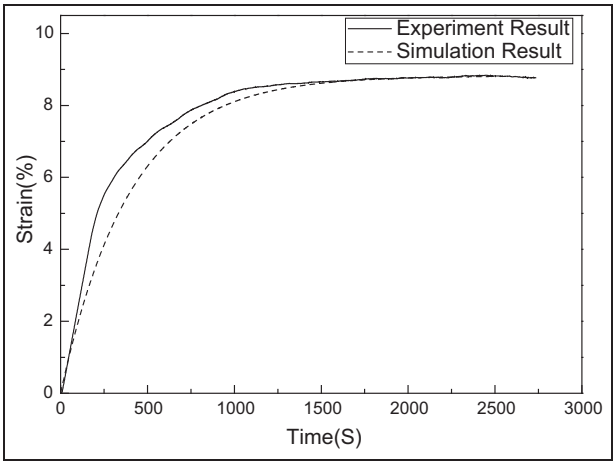

Figure 11. Comparisons with simulation results using creep experiment results at 348 K and 0.05 MPa.

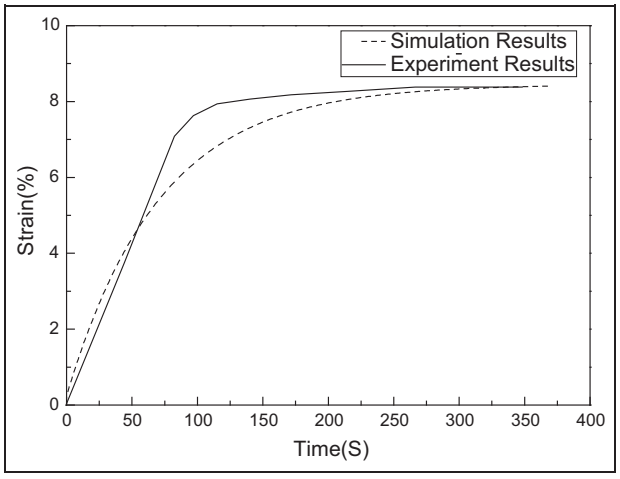

Figure 12. Comparisons with simulation results using creep experiment results at 360 K and 0.05 MPa.

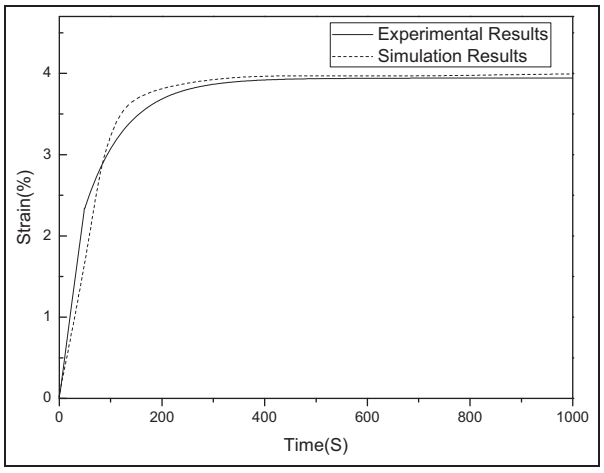

Figure 13. Comparisons with simulation results used creep experiment results at 368 K and 0.01 MPa.

The comparisons between the simulation and experiment results during cooling under a constant strain (30%) process are shown in Figure 14. At the beginning of cooling process, the stress used for maintaining pre-strain increased slowly and the stress was about 0.32 MPa at 381 K. When the temperature reached 334 K, the stress grew rapidly and nonlinear. The ultimate value of stress was 6.2 MPa at 302 K.

Recovery experiment under a constant temperature

In Figure 15, the recovery process at 343 K of SMP was tested. When the pre-stress was removed at 3580 s, the pre-strain deduced sharply and the strain energy was released. But due to low temperature, one part of pre-strain and energy in the material were stored. So, the deformed SMP could not recover to its original shape except at a higher temperature or with a plenty of time. Using equations (14) and (24), the simulated results during the loading and recovery processes were obtained.

In addition, the recovery process at 360 K was also conducted and the experimental results are also shown in Figure 16. As Figure 16 indicates, the deformed specimen can recover to its original shape completely at a high temperature (360 K) in a shorter period of time. Besides, the simulated results were also obtained based

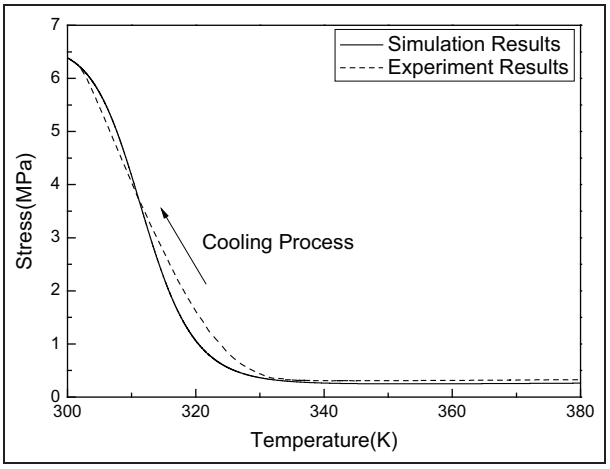

Figure 14. Comparisons with simulation results using the experiment results of cooling under a constant strain (30%).

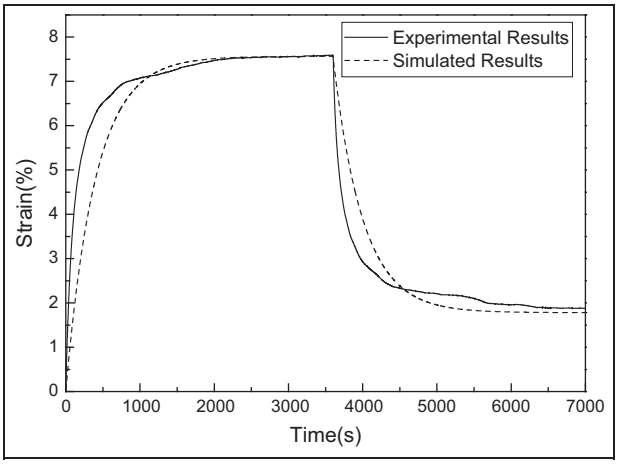

Figure 15. Comparisons with simulation results using recovery experiment results at 343 K.

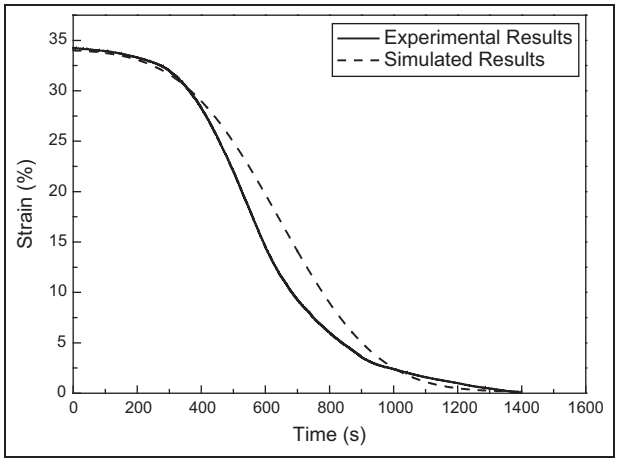

Figure 16. Comparisons with simulation results using recovery experiment results at 360 K.

on equation (24). Through the comparison between the simulated and experimental results, the constitutive model built in this article can describe the recovery process of SMP precisely.

Conclusion

The key of this article is to capture the SME of SMP. Equation (16) explains the mechanism of phase transition and multi-SMEs. For simplicity, SMP was divided into two parts: frozen phase and active phase while the strain was composed of several parts: the mechanical strain in frozen and active phases, storage strain, and thermal expansion strain. Here, the storage strain is the crucial element of SME. In addition, a normal distributed model was used to characterize the volume fraction which is a key factor of equations (16) and (18). Through creep and retardation experiments, the retardation and relaxation time of frozen and active phases were obtained directly or indirectly. Through comparison with the experimental results, the constitutive model established in this article can describe the SME and mechanical behaviors of SMP accurately.

Acknowledgement

This work was supported by the National Natural Science Foundation of China (Grant No 11225211).

Declaration of conflicting interests

The authors declared no potential conflicts of interest with respect to the research, authorship, and/or publication of this article.

Funding

This research received no specific grant from any funding agency in the public, commercial, or not-for-profit sectors.

References

Baghani M, Naghdabadi R, Arghavani J, et al. (2012) A thermodynamically-consistent 3D constitutive model for shape memory polymers. *International Journal of Plasticity* 35: 13–30.

Barot G, Rao IJ and Rajagopal KR (2008) A thermodynamic framework for the modeling of crystallizable shape memory polymers. *International Journal of Engineering Science* 46: 325–351.

Basit A, L'Hostis G and Durand B (2012) Multi-shape memory effect in shape memory polymer composites. *Materials Letters* 74: 220–222.

Behl M and Lendlein A (2007) Actively moving polymers. *Soft Matter* 3: 58–67.

Chen J, Liu L, Liu Y, et al. (2014) Thermoviscoelastic shape memory behavior for epoxy-shape memory polymer. *Smart Materials and Structures* 23: 055025.

Chen Y-C and Lagoudas DC (2008a) A constitutive theory for shape memory polymers. Part I. *Journal of the Mechanics and Physics of Solids* 56: 1752–1765.

Chen Y-C and Lagoudas DC (2008b) A constitutive theory for shape memory polymers. Part II. *Journal of the Mechanics and Physics of Solids* 56: 1766–1778.

Diani J, Gilormini P, Frédy C, et al. (2012) Predicting thermal shape memory of crosslinked polymer networks from linear viscoelasticity. *International Journal of Solids and Structures* 49: 793–799.

Fei G, Li G, Wu L, et al. (2012) A spatially and temporally controlled shape memory process for electrically conductive polymer–carbon nanotube composites. *Soft Matter* 8: 5123–5126.

Ghosh P and Srinivasa AR (2013) A two-network thermomechanical model and parametric study of the response of shape memory polymers. *Mechanics of Materials* 60: 1–17.

Guo X, Liu L, Liu Y, et al. (2014) Constitutive model for a stress- and thermal-induced phase transition in a shape memory polymer. *Smart Materials and Structures* 23: 105019.

Hu J, Zhu Y, Huang H, et al. (2012) Recent advances in shape-memory polymers: structure, mechanism, functionality, modeling and applications. *Progress in Polymer Science* 37: 1720–1763.

Leng J, Lan X, Liu Y, et al. (2011) Shape-memory polymers and their composites: stimulus methods and applications. *Progress in Materials Science* 56: 1077–1135.

Liu Y, Du H, Liu L, et al. (2014) Shape memory polymers and their composites in aerospace applications: a review. *Smart Materials and Structures* 23: 023001.

Liu Y, Gall K, Dunn ML, et al. (2006) Thermomechanics of shape memory polymers: uniaxial experiments and constitutive modeling. *International Journal of Plasticity* 22: 279–313.

Long KN, Dunn ML and Jerry Qi H (2010) Mechanics of soft active materials with phase evolution. *International Journal of Plasticity* 26: 603–616.

Meng H and Li G (2013) A review of stimuli-responsive shape memory polymer composites. *Polymer* 54: 2199–2221.

Meng Q and Hu J (2009) A review of shape memory polymer composites and blends. *Composites Part A: Applied Science and Manufacturing* 40: 1661–1672.

Nguyen T, Jerryqi H, Castro F, et al. (2008) A thermoviscoelastic model for amorphous shape memory polymers: incorporating structural and stress relaxation. *Journal of the Mechanics and Physics of Solids* 56: 2792–2814.

O'Connell PA and McKenna GB (1999) Arrhenius-type temperature dependence of the segmental relaxation below T_g. *The Journal of Chemical Physics* 110: 11054.

Ratna D and Karger-Kocsis J (2007) Recent advances in shape memory polymers and composites: a review. *Journal of Materials Science* 43: 254–269.

Shim J and Mohr D (2011) Rate dependent finite strain constitutive model of polyurea. *International Journal of Plasticity* 27: 868–886.

Shojaei A and Li G (2013) Viscoplasticity analysis of semicrystalline polymers: a multiscale approach within micromechanics framework. *International Journal of Plasticity* 42: 31–49.

Srivastava V, Chester SA and Anand L (2010) Thermally actuated shape-memory polymers: experiments, theory, and numerical simulations. *Journal of the Mechanics and Physics of Solids* 58: 1100–1124.

Tan Q, Liu L, Liu Y, et al. (2014) Thermal mechanical constitutive model of fiber reinforced shape memory polymer composite: based on bridging model. *Composites Part A: Applied Science and Manufacturing* 64: 132–138.

Tobushi H, Hashimoto T, Hayashi S, et al. (1997) Thermomechanical constitutive modeling in shape memory polymer of polyurethane series. *Journal of Intelligent Material Systems and Structures* 8: 711–718.

Tobushi H, Okumura K, Endo M, et al. (2001) Thermomechanical properties of polyurethane-shape memory polymer foam. *Journal of Intelligent Material Systems and Structures* 12: 283–287.

Wei ZG, Sandstroröm R and Miyazaki M (1998) Shape-memory materials and hybrid composites for smart systems. Part I: shape-memory materials. *Journal of Materials Science* 33: 3743–3762.

Westbrook KK, Kao PH, Castro F, et al. (2011) A 3D finite deformation constitutive model for amorphous shape memory polymers: a multi-branch modeling approach for nonequilibrium relaxation processes. *Mechanics of Materials* 43: 853–869.

Xie T (2010) Tunable polymer multi-shape memory effect. *Nature* 464: 267–270.

Xu B, Fu YQ, Ahmad M, et al. (2010) Thermo-mechanical properties of polystyrene-based shape memory nanocomposites. *Journal of Materials Chemistry* 20: 3442–3448.

Yu K, Liu Y and Leng J (2014) Shape memory polymer/CNT composites and their microwave induced shape memory behaviors. *RSC Advances* 4: 2961–2968.

Yu K, Westbrook KK, Kao PH, et al. (2013) Design considerations for shape memory polymer composites with magnetic particles. *Journal of Composite Materials* 47: 51–63.

Yu K, Xie T, Leng J, et al. (2012) Mechanisms of multi-shape memory effects and associated energy release in shape memory polymers. *Soft Matter* 8: 5687–5695.

Zhang P and Li G (2013) Structural relaxation behavior of strain hardened shape memory polymer fibers for self-healing applications. *Journal of Polymer Science Part B: Polymer Physics* 51: 966–977.